

DESIGN METHODOLOGY FOR SEISMIC UPGRADING OF SUBSTANDARD REINFORCED CONCRETE STRUCTURES

GEORGIA E. THERMOU*

*PhD Candidate, Civil Engineering Department
Demokritus University of Thrace, Greece*

STAVROULA J. PANTAZOPOULOU[§]

*Professor, Civil Engineering Department
Demokritus University of Thrace, Greece*

AMR S. ELNASHAI[#]

*Willett Professor, Civil Engineering Department
Director, Mid-American Earthquake Center
University of Illinois at Urbana-Champaign, USA*

Received (received date)

Revised (revised date)

Accepted (accepted date)

This paper presents a design methodology for seismic upgrading of existing reinforced concrete (RC) buildings. The methodology is based on the modification of the deflected shape of the structure so as to achieve a near-uniform distribution of interstorey drift along the building height, thereby eliminating damage localization. Yield point spectra are utilized for the definition of demand and a direct displacement-based design approach is implemented. The fundamental steps of the method are described in detail, including a systematic evaluation of assumptions and limitations. A full-scale tested structure is used as a case study for assessment and verification of the proposed methodology. Alternative retrofit scenarios are set according to target response and performance levels. The role of the target deflected response shape and its influence on the outcome of the retrofit strategy is investigated. The viability of the alternative retrofit scenarios is studied for different ground motions including near-fault earthquake records.

Keywords: Retrofit strategy, seismic upgrading, rehabilitation, displacement-based design

1. Introduction

Seismic evaluation of the existing building stock has become a recognised priority after damage and collapse of many reinforced concrete structures during recent earthquakes. Today, there is a concerted international focus on reduction of seismic risk through assessment and rehabilitation programs to upgrade buildings that are deemed inadequate with regards the level of seismic protection they provide to the public. With the

* Reinforced Concrete Laboratory, Vas. Sofias 12, Xanthi 67100, Greece, e-mail: gthermou@civil.duth.gr

[§] Reinforced Concrete Laboratory, Vas. Sofias 12, Xanthi 67100, Greece, e-mail: pantaz@civil.duth.gr

[#]2129e Newmark Laboratory, 205 North Mathews Avenue, Urbana, Illinois 61801, USA, e-mail: aelnash@uiuc.edu

experience gained through application of various intervention methods and advancements in material technology, practical guidelines are already under development in code format.

Establishing an optimum retrofit strategy is a complex procedure that depends on several technical and socio-economical parameters. Here rehabilitation objectives are set considering requirements for acceptable structural performance and the structural characteristics of the existing building (reinforcement detailing, material strengths). Alternative retrofit scenarios that comply with various performance targets may be established depending on selective or overall modification of stiffness, strength and ductility [Thermou *et al.*, 2004]. Retrofitting should take into account the capacity of the existing foundation system and the limited deformation capacity of non-structural components. A combination of global and/or local intervention methods may be employed depending on the deficiencies of the existing building and the rigor of the post-intervention performance objective.

The main objectives of rehabilitation are to modify the structural response by prioritizing of failure modes and correct any deficiencies related to localization of damage. At the structural level, damage may be quantified by the amount of lateral drift. Performance objectives that define the various structural limit states ranging from “continued operation”, to “collapse”, may also be related directly to lateral deformation. Therefore the conceptual framework of displacement-based design approach is compatible with the stated objectives of retrofitting.

Objective of this paper is to present the milestone steps and verification applications of a design strategy for seismic upgrading of existing RC buildings. A key step in the proposed methodology and a distinguishing feature from other displacement-based proposals [such as SEAOC, 1995; Freeman, 1998; Priestley and Kowalsky, 2000; Fajfar, 2000] is to mitigate damage localization through controlled modification of the lateral response shape of the building. Depending on the structural system type and on the diagnosed deficiencies of the initial condition of the structure, target vibration response shapes may be selected ranging from a shear-type to a flexural profile. To effect a pre-selected target response shape that optimizes interstorey drifts in all floors a weighted distribution of added stiffness along the building height is required. Procedures to modify the available stiffness are developed [Thermou *et al.*, 2004, 2005]. Because the response is considered in the elastic range, stiffness is proportional to the flexural strength of reinforced concrete members. Thus, modification of stiffness is also accompanied by a commensurate change in the strength at yielding of the structural system.

The yield point spectrum format is utilized for definition of demand at yield [Aschheim and Black, 2000]. Members to be retrofitted are designed in order to supply the required stiffness and interstorey drift as dictated by the selected target response shape and the target drift at yield. The approach adopted for the design at member level is based on the direct displacement-based design principles as presented by Moehle [1992]. The ICONS Project (Innovative seismic design CONcepts for new and existing Structures

Project) frame which was tested at full-scale in European Laboratory for Structural Assessment (ELSA) [Pinto *et al.*, 2002] is used as a case study for practical implementation of the proposed retrofit design methodology. Alternative retrofit options are investigated and the response to various ground motions is studied. The impact of near-fault ground motions on the response of the retrofitted structure is studied.

2. Weighted Distribution of Stiffness for Lateral Drift Control

With the seismic demands expressed in spectral coordinates, design force and displacement correspond to the associated single degree of freedom system that represents the major contribution to the structural response. To perform the transformation from a Single- to a Multi-Degree-of-Freedom (SDOF, MDOF) system and vice versa a vibration shape is required; if the fundamental shape is used to conduct the transformation, then calculations are reliable provided the response stays within the elastic range. To satisfy the latter, demand at yield (initiation of the elastic response range) is referred to as a benchmark point in the present analysis. For the latter reason the Yield Point Spectrum (YPS) format was used to quantify the intensity of seismic demands [Aschheim and Black, 2000]. Yield Point Spectra are inelastic constant ductility Acceleration Displacement Response Spectra (ADRS) spectra ($\mu=\Delta_u/\Delta_y$) with the abscissa corresponding to the yield displacement, Δ_y , the ordinate corresponding to the yield strength coefficient, C_y and the radial lines to the period, T (Fig. 1(a)). Yield Point Spectra can be generated from either a code-based format or a site-specific record. This is a graphical procedure; to construct the YPS from the elastic spectra, the hysteretic response is required, relating the force reduction factors, R , with the ductility, μ , as a function of period, T (R - μ - T relationships).

With the aid of the YPS the required stiffness of the Equivalent SDOF (ESDOF) is selected to match a target drift at the point of yielding (Fig.1(a)). The next step is modification of the building response so as to match the pre-selected target deflection shape by pertinent distribution of the added stiffness to the individual floors. To meet this objective the added stiffness is distributed along the height of the building according to a vector of weighting factors, w , which is unique for the given structure and the selected target shape (Fig.1(b)). The stiffness distribution is meant to correct localization of damage by targeting a pre-selected distribution of *interstory drift* heightwise in the structure.

To derive the weighting factors Rayleigh's approximate method of free vibration analysis is used for simplicity and immediate results. The underlying concept is conservation of energy during a period of free vibration through the cyclic conversion of strain energy to kinetic energy and vice-versa. Results of this type of analysis are directly related to the selection of the vibration shape; the true vibration shape converges upon iteration to simultaneously satisfy force equilibrium and the requirement for conservation of energy. The work-equivalent stiffness is obtained from the total strain energy statement, and comprises contributions of the deformable elements in all floor levels; strain energy is associated with translational inter-storey drift for shear framed

structures, but it depends on tangential inter-storey drift in flexural framed structures. In the general case the displacement profile of a structure under lateral load falls between the flexural-type and the shear-type bounds, depending on the relative stiffness of beams and columns. As the vibration shape changes and shifts from the shear to the flexural profile, the influence of the tangential component of drift increases.

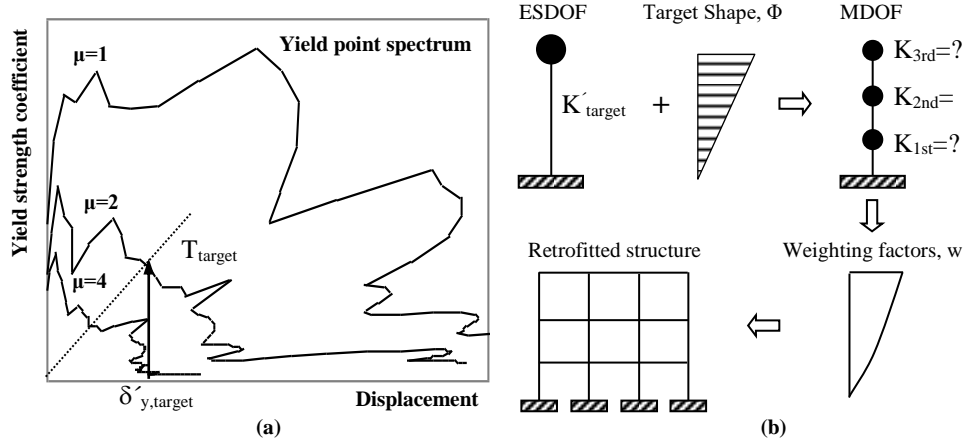


Fig. 1. Yield point spectrum and fundamentals of the proposed retrofit design methodology.

In Table 1, expressions for determining the weighting factor and stiffness component of j^{th} floor for shear-type structures are given. The symbol i refers to number of the floor, n to the total number of floors, K' is the stiffness of the Equivalent SDOF system.

Table 1. Equations for the triangular and parabolic response shape.

Triangular shape		Parabolic shape	
Φ_j	j/n	$1/n^2 j (2n - j)$	
$\Delta\Phi_j$	$1/n$	$2/n^2 (n - j + 0.5)$	
w_j	$\frac{\sum_{i=j}^n i}{\sum_{i=j}^n i^2}$	$\frac{\sum_{i=j}^n i(2n-i)}{\left[\frac{\sum_{i=1}^n i(2n-i)}{(n-i+0.5)_{i=1}} + \dots + \frac{\sum_{i=n-1}^n i(2n-i)}{(n-i+0.5)_{i=n-1}} + 2n^2 \right] (n-i+0.5)_{i=j}}$	
K_j	$w_j \cdot n^2 \cdot K'$	$0.5 \cdot n^4 \cdot \frac{\sum_{i=j}^n i(2n-i)}{\sum_{i=1}^n (i(2n-i))^2 (n-i+0.5)_{i=j}} \cdot K'$	

3. Description of the proposed methodology

The steps of the proposed design methodology are presented as follows:

Step 1: Assessment of the existing building – Evaluating the deficiencies of the structural system is required both at the local and global level. Key characteristics that identify global deficiencies are:

- (i) the fundamental period estimated from gross stiffness properties multiplied by $\sqrt{2}$, as compared with benchmark values for frame buildings ($0.1n$) and wall-type buildings respectively ($0.05n$), where n the number of stories
- (ii) degree of coupling between torsional and translational mode shapes
- (iii) magnitude of coefficient θ used by the Codes to identify sway frames
- (iv) estimated drift at yield (if excessively higher than 0.5%)
- (v) geometric ratios of the structure such as the floor area ratio of reinforced concrete elements being below 1%
- (vi) vertical irregularities that may be readily identified from the response shape through the iterative Rayleigh method (for cracked stiffness, EI_y). Concentration of inelastic deformation (localization) at a particular floor level is expected to occur whenever ID demand exceeds the ID capacity; most often this correlates with irregular distribution of either mass or stiffness along the height of the building. Gravity load designed buildings follow the strong-beam weak-column design philosophy and for this reason the relative strengths of beams, columns and joints need be checked. Detailing in old construction practice is negligible and hence sparse confining reinforcement and short anchorage lengths represent an additional weak link, the significance of which, however, may be controlled through local interventions.

Step 2: Determination of target drift at yield – The *target drift at yield* ($\delta'_{y,target}$) is determined for the ESDOF system. In case of frame-type structural systems a value of 0.50% is satisfactory. For RC wall-type structures a value of 0.25% is stipulated. For mixed type systems a value between 0.25% - 0.50% may be taken. An alternative economic solution would be to correct the response shape without any significant modification to the structural characteristics of the original frame. In that case, members identified in need of retrofit, would be those most affected by localization of failure in the original frame. Interventions are very limited since the objective of this “Lower bound solution” is to correct and not to modify. The deflected response shape is the outcome of the retrofit design procedure.

Step 3: Selection of a target response shape and ductility level – The structure is considered to respond nearly in a single mode. If the retrofit objective is to achieve a uniform distribution of damage along the height of the building, then a triangular response shape may be selected. A more relaxed shape may be used as well depending on the tolerance of damage localization in a single floor as well as the structural type of the building (note that the other extreme is a soft story mechanism whereby all damage occurs in a single floor). The selection of the ductility level of the retrofitted structure depends on experience from structural systems of the type considered, as to how much reliable ductility and deformation capacity may be relied upon after retrofit. A ductility value (μ_δ) between 2 and 3 may be considered achievable for retrofitted buildings. Note

that a ductility level of 3 is the upper limit suggested and it is seen that in the majority of the cases is hardly achievable. At the end of the redesign procedure the retrofitted building should have at least the selected level of ductility. The ductility level may be selected in order to correspond to a particular performance level.

Step 4: Definition of stiffness demand through YPS – The *target stiffness* of the ESDOF system (K'_{target}) is defined by employing the yield point spectrum representation. After the transformation of the ESDOF to the MDOF, the stiffness of the MDOF is determined and distributed along the height of the building according to adequate weighting factors [Thermou *et al.*, 2004, 2005], w_i , related to the response shape selected in Step 3.

Step 5: Decision on the vertical members to be retrofitted – The criterion utilized for determining which vertical members are going to be retrofitted in the j^{th} floor is satisfaction of the *target interstory drift at yield* ($ID_{y,j}$). This depends on the target global drift at yield ($\delta_{y,\text{target}}$), the target response shape (Φ), and the storey height (h_{st}). Elements within a single floor that yield at interstory drift levels significantly greater than the target value ought to be strengthened. In this way, the dispersion of the various levels of relative drift at which vertical members of the lateral load resisting system in a single floor would yield is reduced. New elements may be added as well, as for example RC walls.

Step 6: Rehabilitation of vertical members - Each member of the j^{th} floor need be designed in order to satisfy the target interstory drift at yield ($ID_{y,j}$). First the cross-sectional dimensions of the retrofitted members (e.g. RC jackets) or of the new added members (e.g. RC walls) are defined. It is established that yield displacement depends on the materials and the geometry of the elements. Simplified rules that relate curvature at yield with the height of the cross-section may be utilized in order to provide a quick estimate of the required cross-section height to achieve the target drift at yield. For example curvature at yield may be expressed as (Priestley and Kowalsky [1998] and Priestley [1998]):

$$\varphi_y = \frac{2.14 \cdot e_{sy}}{h_j} \pm 10\% , \text{ for rectangular columns} \quad (3.1a)$$

$$\varphi_y = \frac{2.25 \cdot e_{sy}}{l_w} \pm 15\% , \text{ for walls with distributed reinforcement} \quad (3.1b)$$

$$\varphi_y = \frac{2.00 \cdot e_{sy}}{l_w} \pm 5\% , \text{ for walls with 0.5\% distributed plus end reinforcement} \quad (3.1c)$$

In case of RC jacketed cross-sections the longitudinal reinforcement, ρ_j , may be defined by the following expression (the derivation is presented in Appendix B):

$$\rho_j = 0.22 \cdot \frac{\ell^3}{E_s \cdot b_j} \cdot \left(K_{m,j} + \frac{P_{m,j}}{h_{\text{st}}} \right) - 0.63 \cdot \frac{P_{m,j}}{b_j \cdot h_j \cdot f_{sy}} + 0.75 \frac{P_{m,j}}{b_j^2 \cdot h_j^2 \cdot f_{sy} \cdot f'_c} \quad (3.2)$$

where $K_{m,j}$ the target member stiffness, $P_{m,j}$ the axial load applied, ℓ the ratio of the storey height h_{st} to the height of the jacketed cross-section h_j , E_s the elastic modulus of steel, f_{sy} the steel yield strength, f'_c the concrete compressive strength and b_j the width of the

jacketed cross-section, Eq. (3.2) provides a direct relationship between the longitudinal reinforcement of the jacketed cross-section and the required member stiffness at yield. The entire floor must satisfy the results of step 4 regarding target floor stiffness ($K_j = \sum K_{m,j}$).

Note that deviations from the target shape may be imperative due to code or construction limitations. The design of the retrofitted cross-sections should comply with code provisions (e.g. minimum bar diameter, percentage of longitudinal reinforcement and jacket thickness in case of RC jackets). Therefore, the member retrofit design is not guided by code limitations only when the target member stiffness exceeds the threshold stiffness that corresponds to the code minimum values. For redundancy, the added floor stiffness that results from the weighted distribution should not be attributed to a single member, but to the majority of the elements of the same floor. If this is not feasible then the retrofit schemes should continue to the level above at the expense of the target shape, however, in no case should the redundancy rule be violated so as to avoid creation of a new scenario of potential failure localization.

Step 7: Check drift at ultimate limit state – After dimensioning and detailing, the drift capacity is evaluated for each retrofitted member, m , at each floor, j . Assuming that all premature failure modes but flexural are suppressed through local interventions at the member level, the demand in curvature is expressed in terms of the displacement demand at ultimate $\delta_{m,j}^u$ as follows:

$$\phi_{m,j}^u = \left(\delta_{m,j}^u - \frac{\phi_{m,j}^y \cdot L_s^2}{3} \right) \left(\frac{1}{L_p \cdot (L_s - L_p/2)} \right) + \phi_{m,j}^y \quad (3.3a)$$

$$L_p = 0.08 \cdot L_s + 0.022 \cdot d_b \cdot f_y \quad (3.3b)$$

where, $\delta_{m,j}^u$ the displacement demand at ultimate given as the product of the ductility level selected in Step 3 and the member drift at yield ($\delta_{m,j}^y$) as defined after the design of the retrofit scheme, L_p the estimated length of the plastic hinge region [Paulay and Priestley, 1992], L_s the distance from the critical section of the plastic hinge to the point of contraflexure (usually taken for simplicity as one-half the free span), f_y the steel stress at yield and d_b the diameter of the longitudinal reinforcement. The formula given for the estimation of the plastic hinge length is an empirical one and attention should be paid in its use since it is incompatible with a series of local particularities of critical regions. The solution scheme is acceptable when the ultimate curvature provided by the member exceeds the demand estimated by Eq. (3.3a).

Step 8: Check overall structural response – The overall structural response is checked at the displacement at ultimate taking into account the final response shape of the retrofitted structure as defined after the design of the retrofit schemes. Second order effects are checked in all stories by evaluating the interstory drift sensitivity coefficient θ given as [Eurocode 8, 1994]:

$$\theta = \frac{P_{tot} \cdot ID_{i,n}^u}{V_{tot} \cdot h_{st}} \quad (3.4)$$

where P_{tot} the total gravity load carried by the vertical elements of the storey considered, $ID_{m,j}^u$ the interstorey drift at ultimate, V_{tot} the total seismic storey shear and h_{st} the storey height. In case that $\theta \leq 0.10$ then second order effects should not be taken into account, otherwise the ductility level should be decreased leading to higher seismic action effects.

3.1. Assumptions and limitations

The methodology presented deals with system-level deficiencies that are associated with irregular distribution along the height of the building of either mass or stiffness. The method assumes that the building responds in a single mode and the main objective is to apply those intervention schemes that will modify the response and mitigate damage localization (e.g. soft-storey mechanisms). Global intervention methods such as RC jacketing or addition of RC walls are the most effective intervention methods for modifying stiffness distribution and controlling lateral drift. Intervention methods at member level are applied as well, dealing with poor reinforcement detailing issues such as insufficient anchorage lengths, poorly confined lap-splices and lack of stirrups in plastic hinge regions.

The demand in stiffness is determined by using constant ductility yield point spectra [Aschheim and Black, 2000]. The yield point spectrum allows definition of demand at yield and therefore there is no need for deformation distribution in the post-yield as in the Capacity Spectrum Method (CSM). Pertinent R- μ -T relationships to specifically address the behaviour of retrofitted structures may be selected to improve the accuracy of the computation of the constant ductility spectra. In this study, the equal displacement rule is adopted for the construction of equal ductility Yield Point Spectra. The authors identify that further investigation is necessary for the validity of this rule in case of retrofitted structures. If the yield point spectra are determined from a site-specific record, then the defined demand (Step 4) is sensitive to the characteristics of the ground motion. Therefore in order to avoid variability in response, it is recommended to use smoothed design spectra in upgrading.

In general, the total interstorey drift comprises both beam and column deformations. In the proposed methodology, the work-equivalent effects of the increase in storey-stiffness are estimated considering only the contribution of the columns; this is applicable to shear-type buildings that feature stiff diaphragms. The result is conservative and is acceptable provided that beam-column connections will nevertheless be capacity-designed in the upgraded system. Retrofitting a beam-column connection is not an easy task from both a structural and an economical point of view. In case of RC jacketing, beam-column connections are retrofitted since the longitudinal reinforcement placed in the jacket passes through holes drilled in the slab and new concrete is placed in the beam-column joint. Beam contributions to the work-equivalent stiffness of the structure may also be included if the strain energy stored owing to the tangential component of drift is considered. This increases as the vibration shape changes and shifts from the shear to the flexural profile.

The proposed design methodology does not consider interaction between the superstructure and the foundation system. The flexibility of the foundation influences the overall structural response with a shift of the global yield displacement and an increase in the effective elastic period of the building.

4. Evaluation of the Proposed Retrofit Design Methodology

To demonstrate practical implementation of the proposed retrofit design framework, the methodology is applied to a full-scale 4-storey RC building model, referred to as ICONS Project frame which was tested at European Laboratory for Structural Assessment (ELSA) laboratory of the Joint Research Center (JRC) in Ispra, Italy [Pihno and Elnashai; 2001, Pinto *et al.*, 2002]. The existing frame is assessed and alternative retrofit strategies are presented.

4.1. Assessment of the existing frame

The frame is representative of old construction and specifically of the construction practice of Southern Europe in the 1950s. It is a 4-storey, 3-bay frame. The story height is equal to 2.7 m and 2 of the 3 bays are 5m wide, whereas the 3rd span is 2.5 m (Fig. 2). Cross-sectional dimensions and detailing of the vertical members are given in Fig. 2. All beams in the direction of loading are 250 mm wide by 500 mm deep, whereas transverse beams are 200 mm wide by 500 mm deep. The solid concrete slab thickness is 150 mm. Materials considered in the design phase were a low strength concrete of nominal strength of $f_{ck}=16$ MPa and smooth longitudinal reinforcing steel of class Fe B22k, with nominal yield strength of $f_{syk}=215$ MPa. Test series were carried out for the determination of concrete compressive strength and steel mechanical characteristics. More information relative to reinforcement detailing and material properties is provided in Pinto *et al.* [2002].

The frame features a number of local and global structural deficiencies. It is a gravity-only designed frame and no specific provisions were considered for seismic detailing and inelastic dissipation mechanisms. Deficiencies at the local level refer to poorly confined lap splices at the base of the first and third floor (700 mm lap splice length) in all four columns, smooth bars that resulted in significant drift due to pullout slip, open stirrups, sparse confining reinforcement and potential column shear failure of the stocky columns of the first (C_{B1}) and second floor (C_{B2}).

The frame was subjected first to a pseudo-dynamic (PsD) test corresponding to 475 years return period (475-yrp) input motion and subsequently to a second PsD test carried out with a 975-yrp input motion. It was apparent from the 475-yrp test that deformation demand concentrated in the 3rd storey. During the 975-yrp test the interstory drift at the third storey increased substantially (ID=2.41%) and the test was stopped after 7.5 secs in order to allow for retrofitting. A strong-beam weak-column strength hierarchy in the beam-column connections of the ICONS frame was confirmed by the full-scale tests. The relative rotation (difference of two adjacent inclinometers) of the slender columns was equal to the absolute rotation (obtained directly from inclinometers) indicating that beams

did not deform and the storey drift was only owing to column deformation [Pinto *et al.*, 2002]. The change of the cross-sectional characteristics of the stocky column between the second and the third floor presented a potential source of localization. In particular, the stiffness at yield of the second storey was 212% greater than the stiffness of the third storey. The contribution of the stocky column to the total floor stiffness was 88% for the second floor and 79% for the third floor (due to staggering of the column cross sectional dimension). The latter difference underlines the significant role of the stocky column to the overall response. The poor performance of lap splices at the bottom of the third storey column enforced the localization between the second and the third column.

Before applying the proposed methodology it was assumed that all premature failure modes but flexural would be suppressed through independent local interventions at the member level (e.g. through jacketing with composite wraps). Therefore the proposed methodology deals with deficiencies at global level that refers to irregular distribution along the height either of stiffness or of mass.

4.2. Implementation of the proposed methodology

The designer may follow different retrofit strategies depending among other parameters on the mandated level of the intervention and the financial objectives of the retrofit effort. The general criteria that need be satisfied are correction of any prevailing vertical irregularities and elimination of mechanisms likely to lead to damage localization. Reduction of vulnerability is another important issue that may be dealt with through modification of the structural system so as to increase the redundancy of the lateral load resisting system. Distribution rather than localization of damage is crucial; otherwise the weakest link will jeopardize the stability of the whole structure.

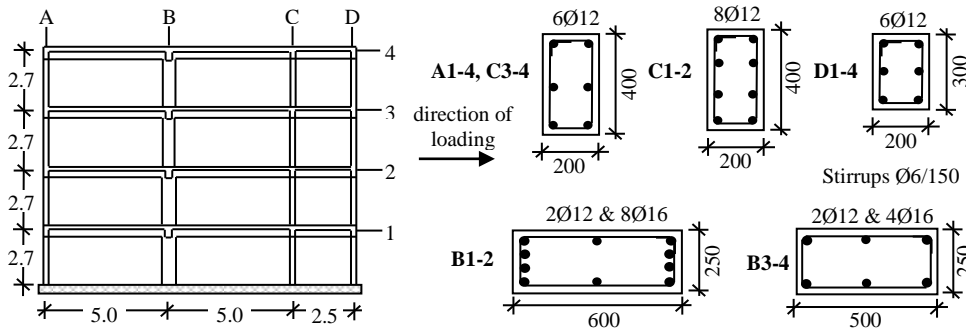


Fig. 2. Configuration and cross-sectional detailing of existing frame.

If the retrofit solution requires a radical modification of behaviour of the existing structure, then a new structural system need be defined for the upgraded system. Motivation for such an option would be an improved distribution of damage amongst members of the same floor, through increased participation of most floor members in the lateral load resisting system. An effort should be made to reduce the dispersion of the

various levels of relative drift at which vertical members in a single floor would yield. In the case study considered a possible retrofit scenario is the following: The target drift at yield is taken equal to 0.5% and the target response shape may vary depending on the distribution of drift along the height. Because this is an old structure with little inherent ductility which is to be increased through the retrofit, a target ductility demand equal to 2 is considered conservative. If an equal distribution of damage is selected along the height of the building, then the triangular response shape is adequate, otherwise for a more relaxed shape (leading to a more economical solution) the parabolic one may be chosen. The retrofit scenario discussed will be referred in the remainder of this work as the “Extensive retrofit proposal”.

An alternative scenario may be adopted which is even more economical and with much less disruption to the function of the building and its occupants. This scenario may be characterized as the “Lower bound solution”, where the main objective is to correct the response shape, i.e. it comprises limited measures needed to mitigate the irregularity in stiffness between the second and the third floor. A similar retrofit solution was adopted in the ICONS frame after the first series of tests. The stocky columns of the third and fourth floor were retrofitted by a strength-only intervention. This was done in order to reduce the flexural capacity differential verified at the third level. More information relative to this application can be found in Pihno [2000], Pihno and Elnashai [2001] and Pinto *et al.* [2002]. Two structural systems may be identified in the building; (i) the stocky columns and (ii) the other vertical members. The stocky columns being stiffer are expected to yield first upon lateral sway. To avoid storey strength degradation, it is required that these columns also possess the necessary ductility so as to follow the deformation of the more flexible members. The average drift at yield for the flexible columns is 1% whereas the average drift at yield for the stocky column is 0.5% which means that the dependable ductility capacity of the stocky column should be at least equal to 2.

Another viable retrofit strategy consists in casting an infill wall to the full width of bay C-D. The existing members, beams and columns C1-4 and D1-4, are incorporated with the latter acting as boundary elements. This retrofit solution modifies substantially the behaviour of the existing frame, altering it from a shear-framed structure to a flexure-framed one. The implementation of the proposed methodology to this retrofit scenario (addition of wall) is presented in Appendix A. Although this retrofit solution is efficient in controlling global lateral drift and thus reducing damage in frame members, presents a drawback related to the adequacy of the existing foundation system to resist the increased overturning moment. Therefore the existing foundation system needs to be checked thoroughly before proceeding to this type of intervention. Moreover, this retrofit solution should consider the intended function of the building. The addition of a wall (i.e. loss of a bay) may be prohibitive in case that the building is located in a commercial street. The economic losses related to its diminished commercial value may render the “extensive retrofit solution” (RC jacketing) more appealing.

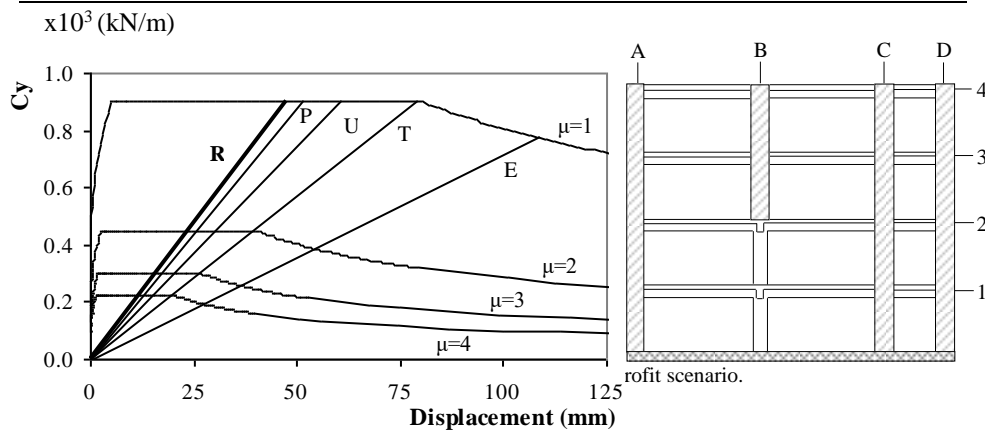
4.2.1 Extensive retrofit proposal

The “Extensive retrofit” aims to a target drift at yield of 0.5% and a ductility displacement ductility level of 2. The demand in all cases is established from the Yield Point Spectra constructed from the elastic spectrum of Eurocode 8 [1994] for soil class B ($p_{ga}=0.36g$) after applying the equal displacement rule. Table 2 presents the demand in terms of interstorey drift at yielding, $ID_{y,j}$, and the stiffness at yielding, $K_{y,j}$, for the triangular and parabolic target response shapes and also for the case of uniform distribution of stiffness heightwise. If a parabolic target shape is used, stiffness demand is increased in the upper floors. Structures susceptible to a soft story formation may be retrofitted in this manner so that interstorey drift localization may be mitigated. The retrofit options selected for the first retrofit scenario are the triangular response shape and the uniform stiffness distribution. In Fig.3, the three retrofit options correspond to the three radial lines, where “T” and “P” stand for triangular and parabolic target response shapes, respectively, whereas “U” corresponds to uniform stiffness distribution. The radial line “E” corresponds to the existing frame.

The extensive retrofit solution is applied to the ICONS frame using the triangular response shape. The target stiffness of each floor is determined according to the weighting factors defined by the equations in Table 1. Deviation of the interstorey drift capacity at yielding from the target value is used as a criterion in order to identify those vertical members in need of retrofit.

Table 2. Alternative retrofit options for the extensive retrofit solution.

Floor	Triangular			Uniform			Parabolic		
	Shape	$ID_{y,j}$	$K_{y,j}$	Shape	$ID_{y,j}$	$K_{y,j}$	Shape	$ID_{y,j}$	$K_{y,j}$
1st	0.25	0.50%	4.52	0.36	0.50%	4.99	0.44	0.50%	5.12
2nd	0.50	0.50%	4.07	0.67	0.44%	4.99	0.75	0.35%	6.17
3rd	0.75	0.50%	3.17	0.89	0.32%	4.99	0.94	0.21%	7.41
4th	1.00	0.50%	1.81	1.00	0.15%	4.99	1.00	0.07%	11.48



Each member is designed for target stiffness and target interstorey drift at yield. Jacketing with reinforced concrete is applied to all columns but C_{B1} and C_{B2} (following the nomenclature of Fig. 2) since these columns are already disproportionately stiff compared to the other vertical members. The drift level that may be attained is controlled by the final height of the jacketed cross-section, whereas the stiffness is more sensitive to the percentage of the longitudinal reinforcement. The concrete selected for the jacket has a compressive strength of $f_{ck}=20$ MPa, whereas longitudinal reinforcing steel with nominal yield strength of $f_{syk}=500$ MPa. Eurocode 2 [1991] is used for the design of the jacketed members. The code minima imposed limitations in the design of the jacketed members and those limitations guided the retrofit solution. The dimensions of the jacketed members along with the reinforcing detailing are shown in Table 3. The stocky column in the first and second floor will be retrofitted by applying Fiber Reinforced Polymer (FRP) jackets to avoid failure in shear.

In Fig. 3, the radial line “R” corresponds to the retrofitted structure. It is observed that the satisfaction of the code minima leads to a stiffer retrofit solution compared to those obtained by the use of the triangular target shape, “T”, and the uniform stiffness distribution, “U”. The shape and stiffness profile of the retrofitted structure are compared to the ones corresponding to the triangular response shape and to the response of the existing frame in Fig. 4(a) and 4(b). It is observed that the localization of damage between the second and third floor has been eliminated.

Table 3. Characteristics of the retrofitted members – Extensive retrofit solution.

Retrofitted frame – Extensive retrofit solution				
Columns	b_j	h_j	$\rho_j (=A_j/(b_j h_j - b_c h_c))$	$\rho_{sw,j}$
C _{A1-4} , C _{C3-4}	500	450	1.04% (6Ø16 & 2 Ø14)	Ø10/100 & Ø10/160
C _{B3-4}	250	600	2.46% (4 Ø14 – Side jacket)	FRP wrapping
C _{C1-2}	500	450	1.00% (4Ø16 & 4 Ø14)	Ø10/100 & Ø10/160
C _{D1-4}	500	400	1.06% (8 Ø14)	Ø10/100 & Ø10/160

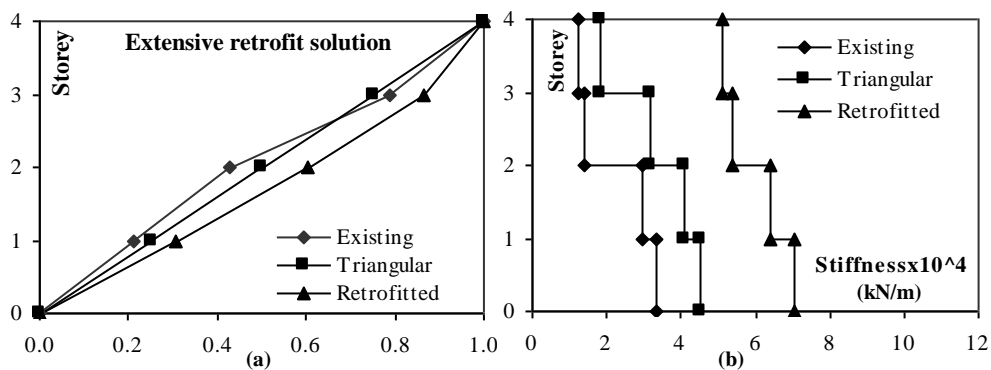


Fig. 4. Shape and stiffness distribution heightwise of the retrofitted structure – Extensive retrofit proposal.

4.2.2 Lower bound solution

The “lower bound solution” is intended to effect modification of the shape of the existing structure only. The triangular response shape may easily be attained by applying reinforced concrete side jacketing to the stocky column of the third and fourth floor (C_{B3} , C_{B4}). The dimension in the strong axis is increased by 100 mm on each side of the section. Longitudinal reinforcement that is added is $2\text{Ø}14$ per side of the column jacketed cross-section. Confinement is provided by FRP wrapping. As illustrated in Fig. 5(b), adopting a triangular target response shape is used results in an abrupt change in the distribution of stiffness between the third and the fourth floor. If this stiffness demand is satisfied by jacketing the stocky column only without any other interventions in the third floor then the lower bound scenario carries the risk of leading to a new source of localization due to the stiffness discontinuity that would prevail in the upper floor. To eliminate this possibility jacketing of the stocky column is extended to the fourth floor as well. The retrofitted frame “R” is shown in the Acceleration Displacement Response Spectrum (ADRS) plot and this solution is slightly differentiated from the target one “T”.

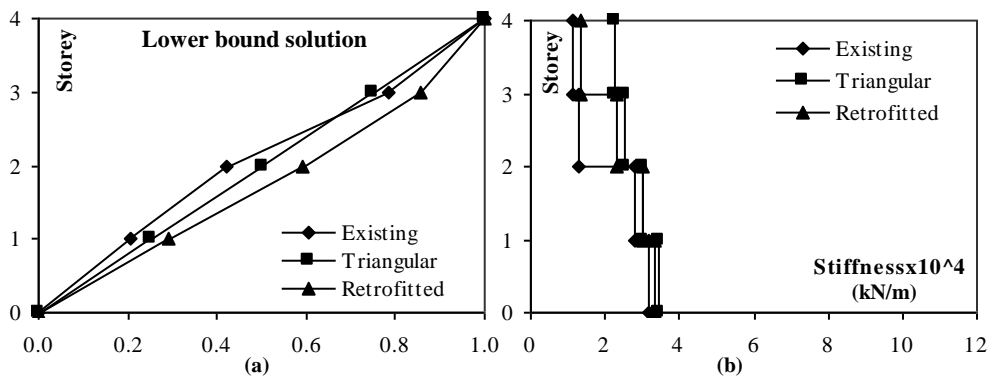
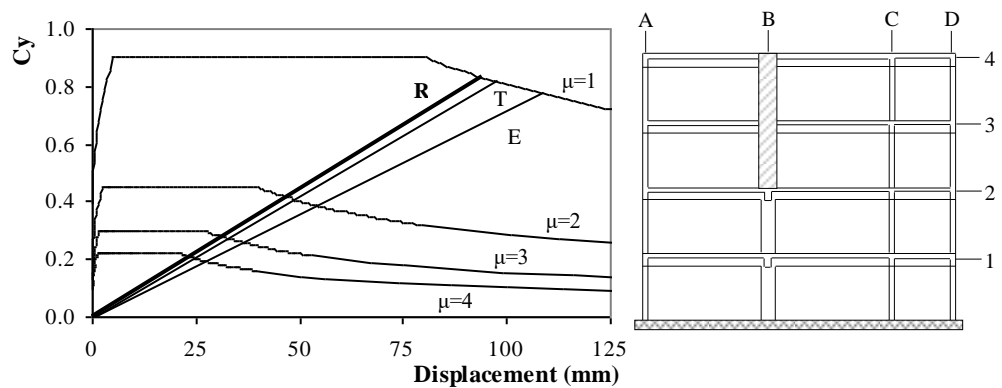


Fig. 5. Shape and stiffness distribution heightwise of the retrofitted structure – Lower bound solution.



5. Assessment of the retrofit options

The two retrofit solutions for the ICONS frame are assessed by performing nonlinear static pushover analyses and a series of inelastic dynamic time-history analyses. Finite models of the retrofitted frames are constructed with the help of ZeusNL, a nonlinear finite element analysis program [Elnashai *et al.*, 2002]. The program is capable of representing the spread of inelasticity within the member cross-section and along the member length utilizing the fiber analysis approach.

Inelastic elements capable of representing progressive cracking and spread of inelasticity are used to model the behaviour of both column and beams of the retrofitted frame. A finer discretization of the plastic hinge regions is used in order to improve the analysis detail. Beam-column joints are assumed rigid and fully-fixed boundary conditions are adopted at the base of the building. Bond slip is not explicitly modelled in the analyses of the various retrofitted options of the frame. This was done so as to isolate and quantify the effects of each alternative retrofitting option on the frame response. Should it be considered, bond slip would modify the response of the existing frame (in the pre-retrofit state) and lead to a softer behaviour. Due to improved confinement provided by jacketing, a large component of drift owing to reinforcement slip is mitigated in strengthened members.

5.1. Response by pushover analysis

Inelastic static pushover analyses are performed to a target drift at ultimate equal to 2% of the building height. The calculated response of the ICONS frame for the two alternative retrofit solutions is plotted against the analytical of the original frame in Fig. 7. A fundamental modification of the response is effected by the extensive retrofit solution, highlighted by the significant increase in stiffness and strength. The steepness of the post-peak softening branch is reduced as compared to the response curves of the existing frame and that of the lower bound solution. This is owing to the reduced influence of second order effects in the behavior of the retrofitted structure. The response curve of the lower bound retrofit solution is almost identical to that of the existing frame; practically, the only difference between the calculated responses, which however is rather decisive, is identified in the lateral response shapes of the two structural systems.

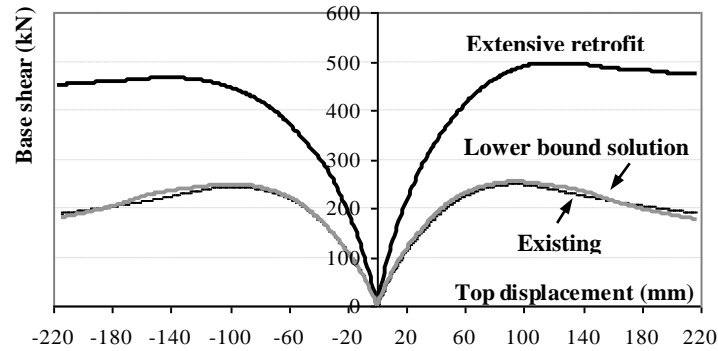


Fig. 7. Calculated base shear vs top displacement for both retrofit solutions.

5.2. Response to earthquake excitation

Inelastic time history analyses are performed for various ground motions in order to assess the level of improvement in the behavior secured through retrofitting. The response of the retrofitted structures was examined by performing dynamic time history analysis for the records that were used in the test and also for near-fault ground motions.

5.2.1. Artificial records

The artificial records that were used in the full-scale test of the ICONS frame are representative of a moderate-high European seismic hazard scenario [Campos-Costa and Pinto, 1999]. The acceleration time histories for seismic events with 475, 975 and 2000 year return periods (referred to hereafter as 475, 975 and 2000) along with their elastic spectra (5% damped) are depicted in Fig. 8. The elastic response spectrum of EC8 used to define the demand in the extensive retrofit solution is also plotted for comparison. The duration of significant excitation in the records is 15 secs and the peak ground acceleration is 0.22g, 0.29g and 0.38g, for the 475, 975 and 2000 year return events, respectively. In the following, the return period is used as an identification code for the record considered.

Calculated displacement histories at the top of the retrofitted frame (extensive retrofit) are plotted in Fig. 9(a) for the group of artificial records. The red line, marked as 2000-All, represents the response of the frame to a sequence of events using records 475, 975 and 2000 in series. Demand is increased as the level of ground motion increases. The interstory drift profiles that correspond to the maximum top displacement are presented in Fig. 9(b) and are compared with the interstory drift profile of the retrofitted frame (R). The interstory drift profile of the retrofitted frame is defined from the critical member of each floor, i.e. the member with the lower level of ductility. In case of the 475 and 975 records, demand is kept well bellow the capacity of the retrofitted frame. The interstory drift demand imposed by the 2000 record reaches the capacity of the retrofitted

frame in the first and second storey, whereas in the other two floors the capacity is higher than the demand. The demand exceeds the capacity of the first and second storey in the 2000-All case, whereas the capacity is greater in the upper two floors. The retrofitted frame is deemed adequate.

The group of artificial records is also applied to the analytical model of the frame retrofitted with the lower bound solution. Calculated displacement time histories at the top of the frame are presented in Fig.10(a). The interstory drift profiles that correspond to the maximum top displacement are presented in Fig.10(b) and are compared to the interstory drift profile of the retrofitted frame (R). The interstory drift profiles that correspond to the maximum top displacement of the retrofitted frame are defined from the member of each floor with the lower level of ductility. The demand imposed by the 475 record is below the capacity of the retrofitted frame. In case of the 975 record the capacity of the first floor is exceeded. In case of the 2000 and 2000-All records, the demand exceeds the capacity in the first two floors whereas the opposite is the case in the upper two floors. The 975 year return period record corresponds to a 10% probability of exceedance in 100 years, which according to SEAOC [1995] is classified as a “Very rare” event.

The response of the frame retrofitted with the lower bound solution is compared to the response of the existing frame as recorded during the test [Pinto *et al.* 2002]. The maximum top displacement and the corresponding interstory drift profiles are compared in Fig. 11(a) and Fig. 11(b), respectively. The blue line, marked as 975-All, represents the response of the frame to a sequence of events using records 475 and 975 in series. The red line which corresponds to the existing frame stops at 22.5 secs because the test was stopped at that time due to the high interstory drift recorded in the 3rd floor. It is observed that the response of the existing and of the lower bound solution frame is identical for the 475 year return period record (first 15 secs). The response continues to be similar up to the peak displacement observed at 22 secs. At that point the response of the lower bound solution frame is differentiated from that of the existing frame. The response of the retrofitted frame appears stiffer. This becomes even clearer if the interstory drift profiles are compared at the maximum top displacement response. The high interstory drift observed in the third level of the existing frame (Fig. 11(b)-red line) is accommodated by the addition of the jackets to the stocky columns of the third and the fourth floor resulting in the blue line profile as depicted in Fig.11(b).

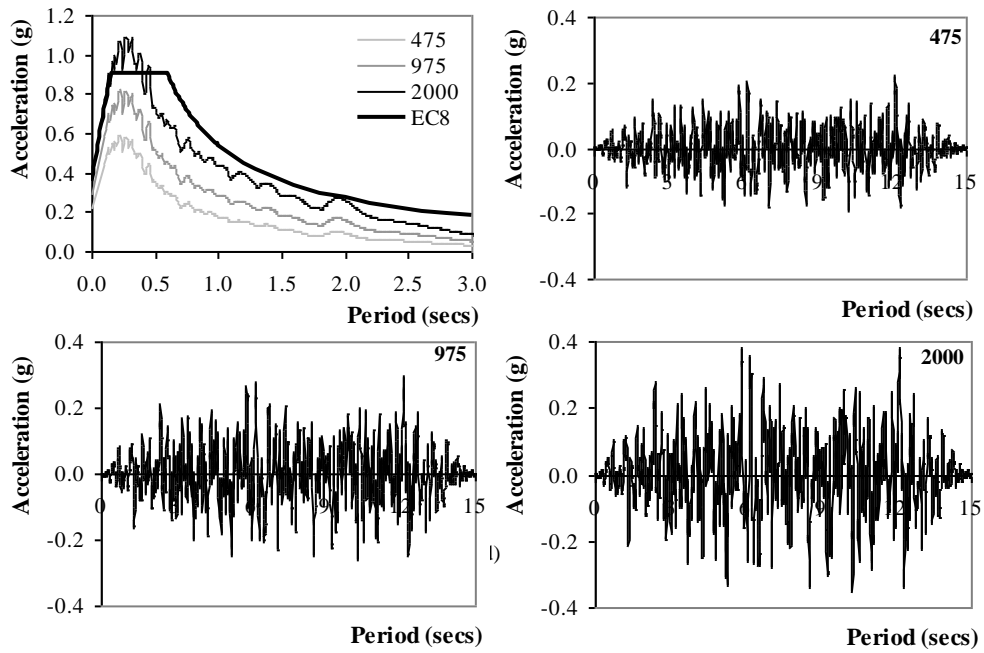


Fig. 8. Elastic response spectra (5% damped) for the group of artificial records.

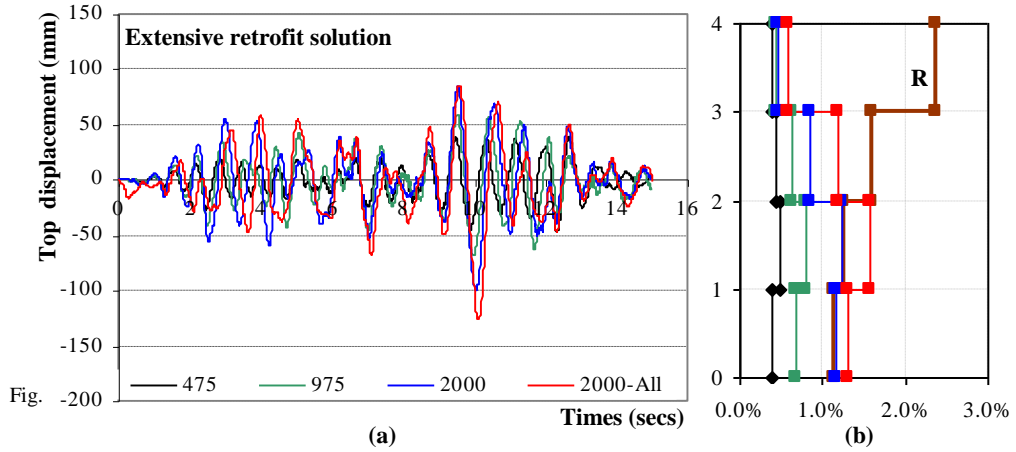


Fig. 9.

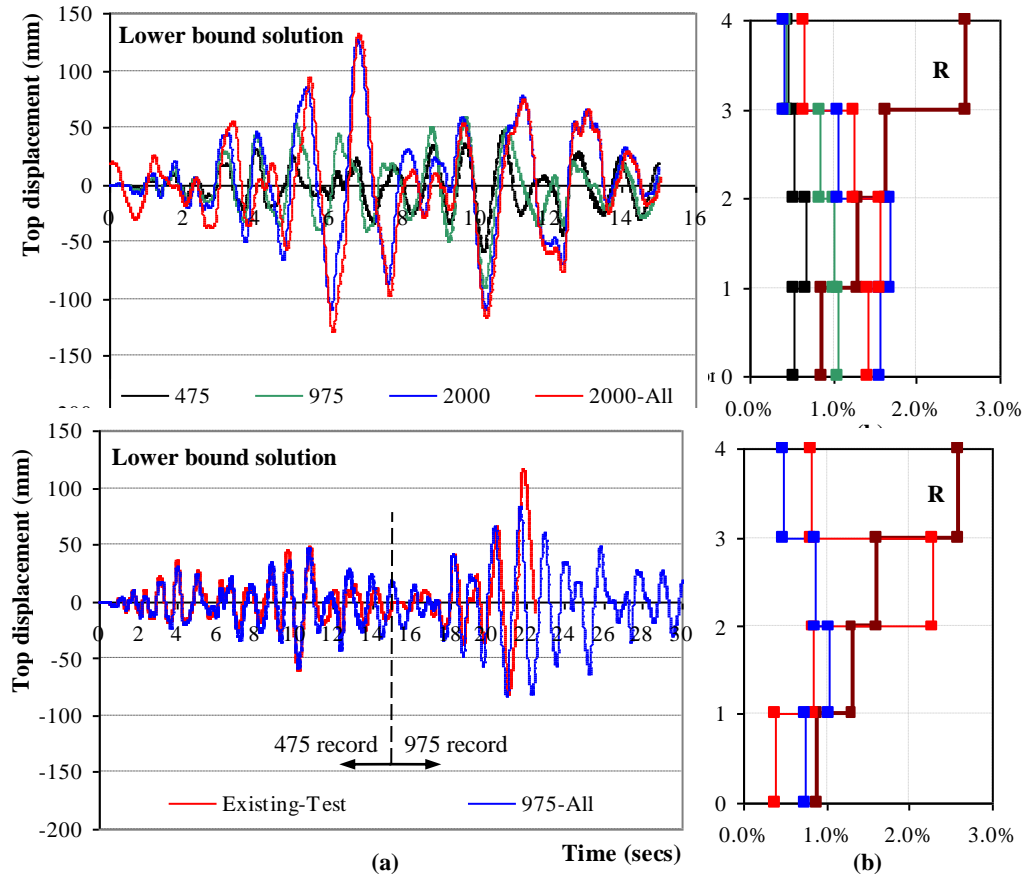


Fig. 11. Comparison of (a) top displacement time histories and (b) interstory drift profiles of the existing frame and the lower bound solution.

5.2.2 Near-fault ground motions

Near-fault ground motions with forward directivity impose a highly non-uniform distribution of ductility demands compared to ordinary ground motions. According to Alavi and Krawinkler [2004], the response of a structure depends on the period of the structure compared to the period of the pulse. Their study demonstrates that when the period of the structure is longer than the period of the pulse then large elastic shear forces are generated in the upper part of the structure. For structures with shorter periods compared to that of the pulse the maximum ductility demands occur in the lower stories regardless of strength.

The response of the retrofitted frames is studied for near-fault ground motions with forward directivity. Two representative recorded ground motions are selected, the Loma Prieta 17/10/89 (LP89SARA.360, $pga=0.504g$) and Northridge 17/1/94 (NR94SYLH.090,

$pga=0.604g$). The ground motions and their elastic response spectra (5% damped) are shown in Fig.12.

Calculated displacement time histories at the top of the frame for the first retrofit scenario are plotted in Fig.13(a). Based on the interstorey drift profile (Fig. 13(b)), the response to the Loma Prieta earthquake is satisfactory since the demand is lower to supply, apart from the second floor where the difference is marginal. The response is differentiated in the case of Northridge earthquake where the displacement demand in the first and second storey increases significantly. It is observed that after the first 8 secs of response the frame has residual deformations. This indicates that stiffness level should be increased and also member ductility should be controlled in the first three storeys.

The lower bound solution is not a viable retrofit option for the near-fault ground motions selected herein. The demand imposed by both near-fault ground motions is very high with the highest interstorey drift demand to be observed in the first and second storey. The interstorey drift profiles of Fig. 14(b) correspond to time step $t_{LP}=7.92$ secs for the Loma Prieta earthquake, $t_N=7.00$ secs for the Northridge earthquake. The top displacement time histories in Fig. 14(a) indicate the low level of lateral strength. The analysis in case of the Northridge earthquake cannot converge and terminates at 8.98 secs.

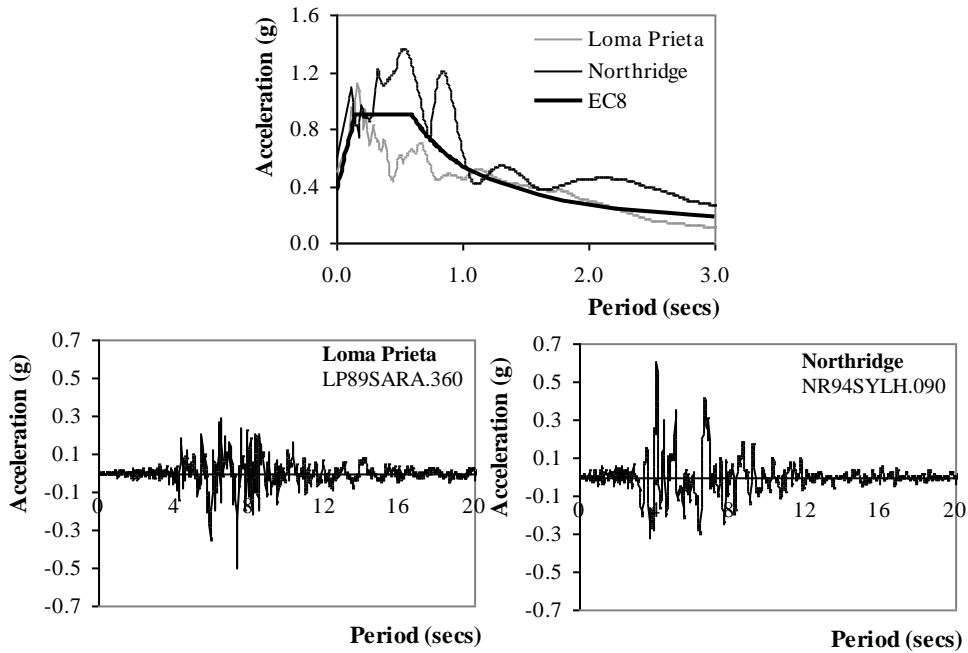


Fig. 12. Elastic response spectra (5% damped) for the group of near-fault records.

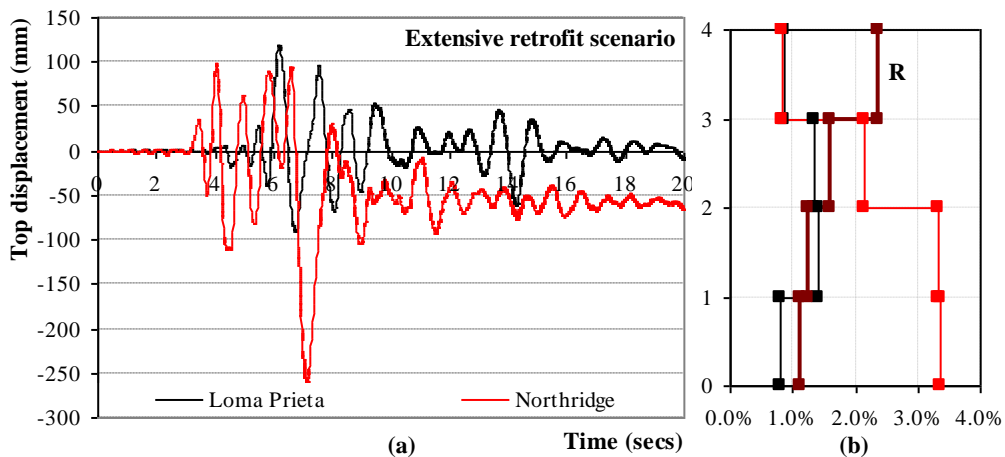


Fig. 13. (a) Top displacement time histories and (b) interstory drift profiles for the extensive retrofit scenario.

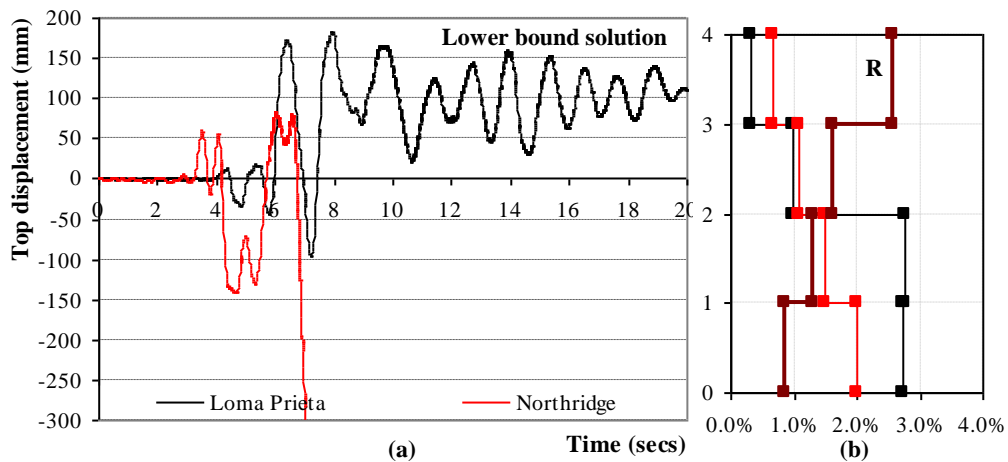


Fig. 14. (a) Top displacement time histories and (b) interstory drift profiles for the lower bound solution.

6. Conclusions

A displacement-based design methodology for rehabilitation of existing reinforced concrete buildings was presented. The central concept of the proposed methodology is modification of the structural properties as required by a weighted distribution of stiffness along the height of the building designed to yield a pre-selected target response shape. In the proposed retrofit design methodology the structure is considered to respond in a single shape, which may be approximated with no loss of generality by the fundamental mode of vibration. Higher mode effects may become important in the post-retrofit structural response of some structural systems, and as such this issue may warrant future extension of the proposed methodology. The yield point spectrum representation is utilized for definition of demand. Members are designed to undergo the deformation demand as required by the target distribution of interstory drift and to reach the required

level of secant-to-yield stiffness. The proposed method is applied to a full-scale tested structure and alternative retrofit solutions are proposed. The effectiveness of the alternative retrofit scenarios is confirmed through dynamic time-history analyses for a variety of strong ground motions including near field records.

7. Acknowledgements

The work presented above was funded by the following organizations:

The Hellenic Ministry of Education and Religious Affairs (Graduate Scholarship HERAKLEITOS)

The General Secretariat for Research and Technology (Project ARISTION)

The European research network “Seismic Performance Assessment and Rehabilitation” (Project SPEAR)

The Mid-America Earthquake Center, a US National Science Foundation Engineering Research Center, funded under grant EEC 97-01785.

Appendix A.

The infill wall is added into bay C-D by incorporating the existing columns C1-4 and D1-4. Two structural systems may be identified in the building; (i) the wall (infilled bay C-D) and (ii) the other vertical members (A1-4 and B1-4). The behaviour of the retrofitted structure is influenced greatly by the presence of the wall. This implies that the target response shape will be of flexural type. The target shape is selected to be $\Phi(x)=1-\cos(\pi x/(2L))$. The demand as in the other cases is established from the Yield Point Spectra constructed from the elastic spectrum of Eurocode 8 [1994] for soil class B ($p_g=0.36g$) after applying the equal displacement rule. The infill wall will have the same geometry along the height of the building. In this case, it can be modeled as a cantilever with constant mass distribution along its height and constant flexural stiffness at yield, EI_y^w . The stiffness of the MDOF is determined with the only unknown the stiffness of the wall at yield.

With the height of the cross-section of the wall determined a priori (length of bay C-D, $l_w=2.7m$), the target drift at yield is taken equal to 0.5% ($\Delta_y=11/40\phi_y L_s^2$), ϕ_y given by Eq. (3.1c) and the target displacement ductility equal to the level of 2. The concrete selected for the infill has a compressive strength of $f_{ck}=20$ MPa, and longitudinal reinforcing steel with nominal yield strength of $f_{syk}=500$ MPa. Eurocode 2 [1991] is used for the design of the wall. According to the code guidelines the existing columns are not adequate to serve as boundary elements and therefore additional boundary elements are necessary (Fig. A1). Attention should be paid in the connection between the existing members and the infill walls. Dowels should be placed between the old and the new components (columns and beams) in order to secure a monolithic connection. The reinforcement detailing of the wall is shown in Fig. A1. The height of the critical region is equal to the height of the first storey $h_{cr}=2.7m$. The stirrups spacing is modified from 100mm within the critical region to 160mm outside the critical region.

The effectiveness of this retrofit solution is assessed by performing pushover and inelastic dynamic analysis for the records presented above. Inelastic static pushover analysis is performed to a target drift at ultimate equal to 2% of the building height. The calculated response of the ICONS frame for the case of adding an infill wall in bay C-D is plotted against the response of the extensive retrofit, the lower bound option and the original frame in Fig. A2. The addition of the infill wall increases substantially the stiffness and strength of the original frame. The base shear of the wall retrofit solution is two times greater than the base shear of the extensive retrofit solution (all the vertical members were jacketed) and 4.4 times greater than the base shear of the lower bound solution. The overturning moment of the wall retrofit solution is 2.2 times greater than the overturning moment of the extensive retrofit solution and 4.3 times greater than the overturning moment of the lower bound solution.

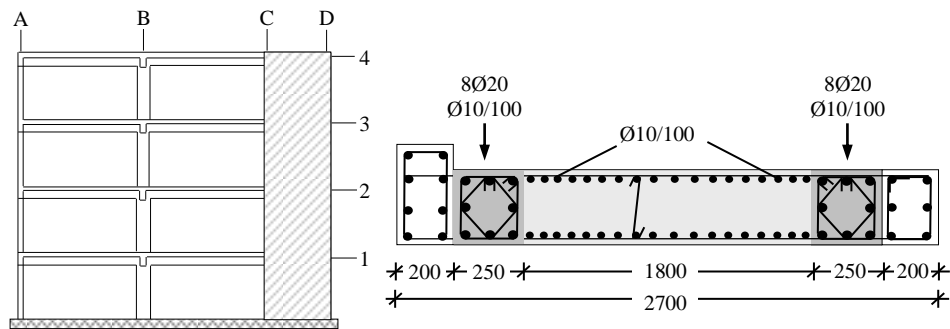


Fig. A1 Configuration of the retrofitted frame and cross-sectional detailing of the infill wall.

The wall retrofit solution is subjected to the artificial records presented above (475, 975, 2000 and 2000-All). Calculated displacement histories at the top of the retrofitted frame (infill wall) are plotted in Fig. A3(a) for the group of artificial records. The interstory drift profiles that correspond to the maximum top displacement are presented in Fig. A3(b) and are compared with the interstory drift profile of the retrofitted frame (R). The interstory drift profile of the retrofitted frame is defined from the critical member of each floor, i.e. the member with the lower level of ductility. In case of the 475 record, demand is kept well below the capacity of the retrofitted frame in the three upper floors, whereas the capacity of the first floor is reached. The interstory drift demand imposed by the 975 record exceeds the capacity of the retrofitted frame in the first storey, whereas in the other floors the capacity is higher than the demand. The demand exceeds the capacity of the first and marginally of the second storey in the 2000 and 2000-All case, whereas the capacity is greater in the upper two floors.

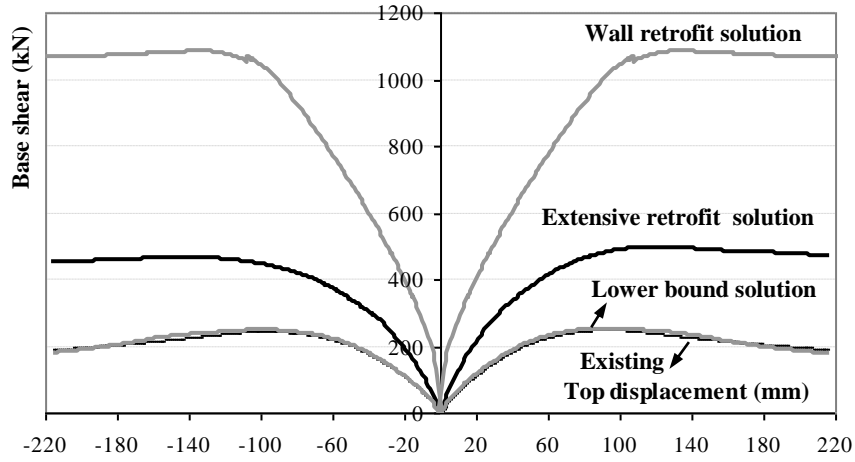
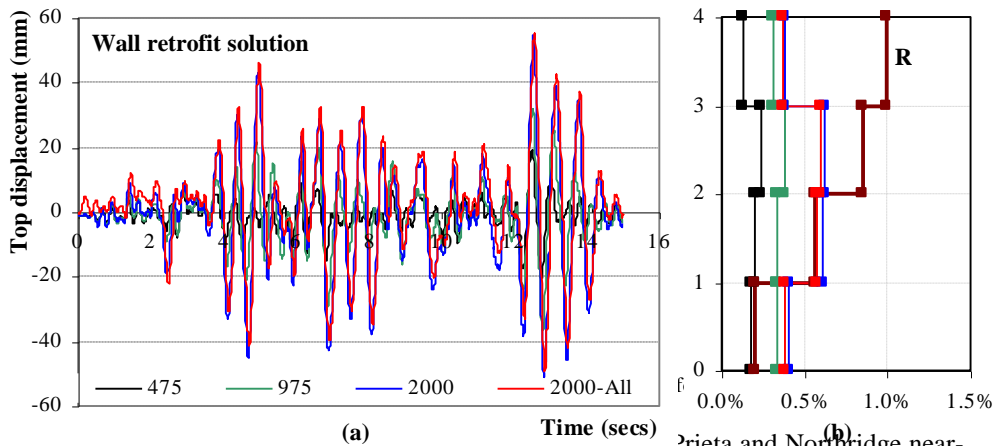


Fig. A2. Calculated base shear vs top displacement for all the retrofit solutions.



ria and Northridge near-fault ground motions. Calculated displacement time histories at the top of the frame for the wall retrofit solution are plotted in Fig. A4(a). Based on the interstory drift profile (Fig. A4(b)), the response to the Loma Prieta earthquake is satisfactory since the demand is lower than the supply, apart from the first floor. The response is differentiated in the case of Northridge earthquake where the displacement demand in all storeys increases significantly. It is observed that after the first 4 secs of response the frame has residual deformations. This indicates that stiffness level should be increased and also member ductility should be controlled in the storeys.

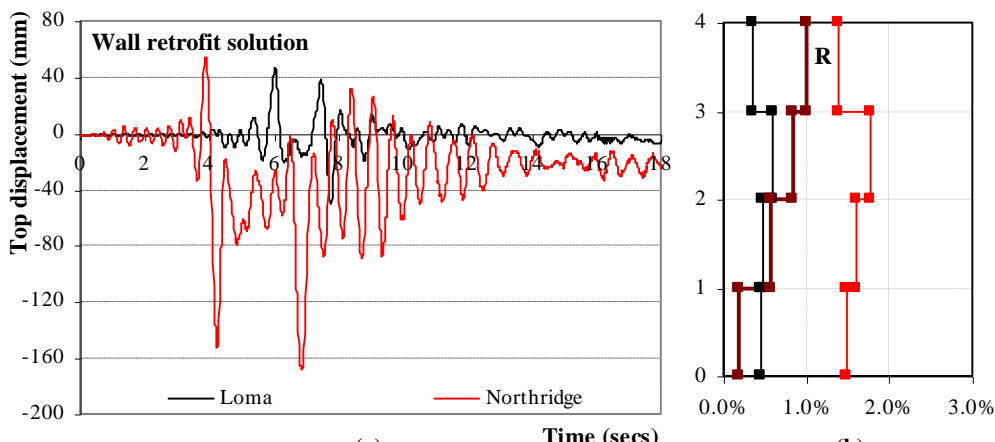


Fig. A4. (a) Top displacement time histories and (b) interstorey drift profiles for the wall retrofit.

Appendix B.

The stiffness at yield of a prismatic member, m , at the j^{th} floor may be given by the following equation:

$$K_{m,j} = \frac{12 \cdot E_c I_y}{h_{st}^3} = \frac{12 \cdot (M_{m,j}^y - P_{m,j} \cdot \Delta_{m,j}^y)}{h_{st}^3 \cdot \varphi_{m,j}^y} \quad (\text{B.1})$$

where $E_c I_y$ the secant flexural stiffness at yield, h_{st} the storey height, $P_{m,j}$ the externally applied axial load, $M_{m,j}^y$ the moment at yield and $\varphi_{m,j}^y$ and $\Delta_{m,j}^y$ the associated curvature and relative displacement. The displacement at yield may be defined by using the stick model which refers to the tip displacement of a cantilever having a length of L_s ($=h_{st}/2$) (for seismic loading the cantilever considered represents the shear span of a member under lateral sway).

$$\Delta_{m,j}^y = \frac{1}{3} \cdot \varphi_{m,j}^y \cdot L_s^2 \quad (\text{B.2})$$

It is assumed that the longitudinal reinforcement of the existing cross-section (core of the jacketed cross-section) does not contribute to the flexural resistance of the jacketed member. In case of poor bond conditions (smooth bars, insufficient lap splices) this approach is on the safe side. In general, this assumption simplifies the design expressions and facilitates design procedure without loss of accuracy. Detailed expressions for the evaluation of the height of the compressive zone of jacketed members are presented in Appendix C. Assuming that the cross-section has equal top and bottom reinforcement, ρ_j , the moment at yield is defined by:

$$M_{m,j}^y = 0.8 \cdot b_j \cdot h_j^2 \cdot f_{sy} \cdot \rho_j + 0.5 \cdot h_j \cdot P_{m,j} - 0.6 \frac{P_{m,j}^2}{b_j \cdot f_c'} \quad (\text{B.3})$$

where ρ_J the top or bottom longitudinal reinforcement of the jacketed cross-section, b_J and h_J the width and the height of the jacketed cross-section respectively, f_{sy} the yield stress of the longitudinal reinforcement, f'_c the concrete compressive strength and $P_{m,j}$ the externally applied axial load.

By introducing Eq. (3.1a), (A.2) and (A.3) into Eq. (A.1) and solving for the longitudinal reinforcement of the jacketed cross-section, the following is obtained:

$$\rho_J = 0.22 \cdot \frac{\ell^3}{E_s \cdot b_J} \cdot \left(K_{m,j} + \frac{P_{m,j}}{h_{st}} \right) - 0.63 \cdot \frac{P_{m,j}}{b_J \cdot h_J \cdot f_{sy}} + 0.75 \frac{P_{m,j}}{b_J^2 \cdot h_J^2 \cdot f_{sy} \cdot f'_c} \quad (\text{B.4})$$

where ℓ the ratio of the story height, h_{st} , to the height of the jacketed cross-section h_J and E_s the elastic modulus of steel.

Appendix C.

The height of the compression zone of the jacketed cross-section, c_y , is estimated from:

$$c_y = A \cdot h_J + \sqrt{(A^2 \cdot h_J^2 + 2 \cdot B \cdot h_J)}, \quad c_y = \xi_y \cdot d_{2J} \quad (\text{C.1})$$

Parameters A and B are defined as:

$$A = -(n-1) \cdot \rho_{sc1} - n \cdot \rho_{sc2} - n \cdot \rho_{wc} \cdot (\delta_{2c} - \delta_{1c}) - (n-1) \cdot \rho_{sJ1} - n \cdot \rho_{sJ2} - n \cdot \rho_{wJ} \cdot (\delta_{2J} - \delta_{1J}) \quad (\text{C.2a})$$

$$B = (n-1) \cdot \rho_{sc1} \cdot d_{1c} + n \cdot \rho_{sc2} \cdot d_{2c} + 0.5 \cdot n \cdot \rho_{wc} \cdot (d_{1c} + d_{2c}) \cdot (\delta_{2c} - \delta_{1c}) + (n-1) \cdot \rho_{sJ1} \cdot d_{1J} + n \cdot \rho_{sJ2} \cdot d_{2J} + 0.5 \cdot n \cdot \rho_{wJ} \cdot (d_{1J} + d_{2J}) \cdot (\delta_{2J} - \delta_{1J}) \quad (\text{C.2b})$$

where b_J and h_J the width and the height of the jacketed cross-section respectively, n the modular ratio E_s/E_c , $\delta_{1c}=d_{1c}/h_J$, $\delta_{2c}=d_{2c}/h_J$, $\delta_{1J}=d_{1J}/h_J$, $\delta_{2J}=d_{2J}/h_J$, $\rho_{sc1}=A_{sc1}/(b_J \cdot h_J)$, $\rho_{sc2}=A_{sc2}/(b_J \cdot h_J)$, $\rho_{sJ1}=A_{sJ1}/(b_J \cdot h_J)$, $\rho_{sJ2}=A_{sJ2}/(b_J \cdot h_J)$, $\rho_{wc}=A_{wc}/[b_J \cdot (d_{1c}+d_{2c}-2c_y)]$, $\rho_{wJ}=A_{wJ}/[b_J \cdot (d_{1J}+d_{2J}-2c_y)]$ (Fig. B1).

Eq. (B.2a) and (B.2b) are applicable in case that no axial load is applied on the jacketed cross-section. Depending on the magnitude of axial load, yielding may occur when either bottom steel reinforcement reaches yield or the compressive concrete strain reaches a certain level ($\epsilon_c=1.8 \cdot f'_c/(E_c \cdot c_y)$). In this case, parameters A and B are modified to parameters A' and B' as:

$$A' = A - \frac{v \cdot f'_c}{\epsilon_{sy} \cdot E_c}, \quad B' = B + \frac{v \cdot f'_c \cdot d_{2J}}{\epsilon_{sy} \cdot E_c} \quad (\text{yielding of tension steel}) \quad (\text{C.3})$$

$$A' = A + 0.55 \cdot v, \quad B' = B \quad (\text{yielding due to compressive strain}) \quad (\text{C.4})$$

where v the dimensionless axial load ($=P_{m,j}/(f_c' \cdot b_j \cdot h_j)$).

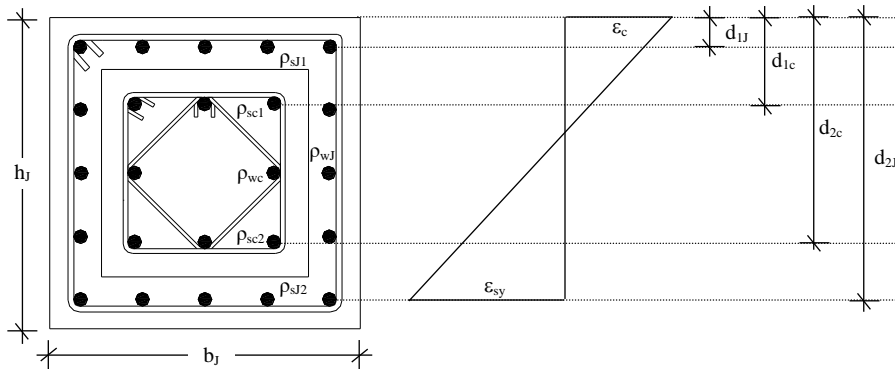


Fig. C1. Jacketed cross-section.

References

- Alavi, B. and Krawinkler, H. [2004] "Strengthening of moment-resisting frame structures against near fault ground motions," *Earthquake Engineering and Structural Dynamics* **33**(6), 707-722.
- Aschheim, M. A. and Black, E. F. [2000] "Yield Point Spectra for seismic design and rehabilitation," *Earthquake Spectra (EERI)* **16**(2), 317-336.
- Campos-Costa, A. and Pinto, A. V. [1999] "European seismic hazard scenarios — An approach to the definition of input motions for testing and reliability assessment of civil engineering structures," JRC Special Publication No. X.99.XX, JRC, Ispra, Italy.
- Elnashai, A. S., Papanikolaou, V. and Lee, D. -H. [2002] ZEUS-NL User Manual, Mid-America Earthquake Center (MAE) Report.
- Eurocode 2 [1991] Design of concrete structures, Part 1. ENV1992-1-1, CEN European Committee for Standardisation. Brussels.
- Eurocode 8 [1994] Design provisions for earthquake resistance of structures, Part 1.1. ENV1998-1-1, CEN European Committee for Standardisation. Brussels.
- Fajfar, P. P. [2000] "A nonlinear analysis method for performance-based seismic design," *Earthquake Spectra (EERI)* **16**(3), 573-592.
- Freeman, S. A. [1998] "The capacity spectrum method as a tool for seismic design," *Proc. of the Eleventh European Conference on Earthquake Engineering, Paris, France*, CD-ROM.
- Moehle, J. P. [1992] "Displacement-based design of RC structures subjected to earthquakes," *Earthquake Spectra* **8**(3), 403-428.
- Paulay, T. and Priestley, M. N. J. [1992] *Seismic Design of Reinforced Concrete and Masonry Buildings* (John Wiley & Sons, Inc., New York).
- Pihno, R. [2000] "Selective retrofitting of RC structures in seismic areas", *PhD Thesis*, Imperial College, London, U.K.
- Pinho, R. and Elnashai, A. S. [2001] "Dynamic collapse testing of a full-scale four story RC frame," *ISET Journal of Earthquake Technology* **37**(SI.4), 143-163.
- Pinto A., Verzeletti G., Molina J., Varum H., Pinho R. and Coehlo E. [2002] "Pseudo-dynamic tests on non-seismic resisting RC frames (bare and selective retrofit frames)," EUR Report 20244EN, JRC, Ispra, Italy.
- Priestley, M. J. N. [1998] "Brief comments on elastic flexibility of reinforced concrete frames and significance to seismic design," *Bulletin, New Zealand National Society for Earthquake Engineering* **31**(4), 246-259.

- Priestley, M. J. N. and Kowalsky, M. J. [1998] "Aspects of drift and ductility capacity of cantilever structural walls," *Bulletin, New Zealand National Society for Earthquake Engineering* **31**(2), 73-85.
- Priestley, M. J. N. and Kowalsky, M. J. [2000] "Direct displacement-based seismic design of concrete buildings", *Bulletin, New Zealand National Society for Earthquake Engineering* **33**(4), 421-444.
- SEAOC [1995] *Performance Based Seismic Engineering of Buildings*, Vision 2000 Committee, Structural Engineers Association of California, Sacramento, California.
- Thermou, G. E., Pantazopoulou, S. J. and Elnashai, A. S. [2004] "Upgrading of RC structures for a target response shape," *Proc. of the Thirteenth World Conference on Earthquake Engineering*, Vancouver, Canada, Paper No 1412.
- Thermou, G. E., Pantazopoulou, S. J. and Elnashai, A. S. [2005] "Design Methodology for seismic upgrading of existing RC structures," *Proc. of the fib Symposium "Keep Concrete Attractive"*, Budapest, Hungary, Paper No 302.